

Quantum phase transitions in the exactly solved spin-1/2 Heisenberg-Ising ladder

Taras Verkholyak^{1,2}, Jozef Strečka²

¹Institute for Condensed Matter Physics, National Academy of Sciences of Ukraine, 1 Svientsitskii Street, L'viv-11, 79011, Ukraine

²Department of Theoretical Physics and Astrophysics, Institute of Physics, P. J. Šafárik University, Park Angelinum 9, 040 01 Košice, Slovak Republic

E-mail: werch@icmp.lviv.ua

Abstract. Ground-state behaviour of the frustrated quantum spin- $\frac{1}{2}$ two-leg ladder with the Heisenberg intra-rung and Ising inter-rung interactions is examined in detail. The investigated model is transformed to the quantum Ising chain with composite spins in an effective transverse and longitudinal field by employing either the bond-state representation or the unitary transformation. It is shown that the ground state of the Heisenberg-Ising ladder can be descended from three exactly solvable models: the quantum Ising chain in a transverse field, the 'classical' Ising chain in a longitudinal field or the spin-chain model in a staggered longitudinal-transverse field. The last model serves in evidence of the staggered bond phase with alternating singlet and triplet bonds on the rungs of two-leg ladder, which appears at moderate values of the external magnetic field and consequently leads to a fractional plateau at a half of the saturation magnetization. The ground-state phase diagram totally consists of five ordered and one quantum paramagnetic phase, which are separated from each other either by the lines of discontinuous or continuous quantum phase transitions. The order parameters are exactly calculated for all five ordered phases and the quantum paramagnetic phase is characterized through different short-range spin-spin correlations.

PACS numbers: 75.10.Jm, 05.30.Rt

Submitted to: *J. Phys. A: Math. Gen.*

1. Introduction

Quantum spin models with competing interactions represent quite interesting and challenging topic for the current research [1, 2]. Such models show many unusual features in their ground-state properties and are very sensitive to the approximative schemes applied to them. An existence of exact solutions is therefore quite important, since they provide a rigorous information about the complex behaviour of frustrated models. However, exact results for such systems are still limited (see [3] and references cited therein). The simplest examples of rigorously solved quantum spin models are the models with the known dimerized [3–6] or even trimerized [7] ground states. Another example represents frustrated quantum spin antiferromagnets in high magnetic fields with the so-called localized-magnon eigenstates (see e.g. [8] for recent review). It should be nevertheless noticed that the aforementioned exact results are usually derived only under certain constraint laid on the interaction parameters and those models are not tractable quite generally.

On the other hand, the exact solutions for some spin- $\frac{1}{2}$ quantum spin ladders with multispin interaction allows to find, besides the ground state, also thermodynamic properties quite rigorously [9, 10]. Exactly solvable models, which admit the inclusion of frustration, can also be constructed from the Ising models where the decorations of quantum spins are included [11, 12]. The decoration-iteration procedure allows one to calculate exactly all thermodynamic properties of the decorated models when the exact solution for the corresponding Ising model is known. The distinctive feature of these models is that the quantum decorations are separated from each other, so that the Hamiltonian can be decomposed into the sum of commuting parts. The eigenstates of the total Hamiltonian are then simply factorized into a product of the eigenstates of its commuting parts.

New findings of the exactly solvable frustrated quantum spin models with non-trivial (not simply factorizable) ground states are thus highly desirable. The present article deals with the frustrated quantum spin- $\frac{1}{2}$ two-leg ladder with the Heisenberg intra-rung interaction and the Ising inter-rung interactions between nearest-neighbouring spins from either the same or different leg. Such a model can be regarded as an extension of the spin- $\frac{1}{2}$ Heisenberg-Ising bond alternating chain, which was proposed and rigorously solved by Lieb, Schultz and Mattis [13]. Alternatively, this model can also be viewed as the generalization of the exactly solved quantum compass ladder [14–16] when considering the Heisenberg rather than XZ-type intra-rung interaction and accounting for the additional frustrating Ising inter-rung interaction. Moreover, it is quite plausible to suspect that the exact results presented hereafter for the spin- $\frac{1}{2}$ Heisenberg-Ising two-leg ladder may also bring insight into the relevant behaviour of the corresponding Heisenberg two-leg ladder, which represents a quite challenging and complex research problem in its own right [17, 18]. The frustrated spin- $\frac{1}{2}$ Heisenberg two-leg ladder have been extensively investigated by employing various independent numerical and analytical methods such as density-matrix renormalization

group [19–22], numerical diagonalization [22–26], series expansion [26], bosonization technique [27–29], strong- and weak-coupling analysis [30–34], valence-bond spin-wave theory [36], variational matrix-product approach [37, 38], and bond mean-field theory [39–41]. Among the most interesting results obtained for this quantum spin chain, one could mention an existence of the columnar-dimer phase discussed in [32, 33] or a presence of the fractional plateau in the magnetization process examined in [22–25, 34].

The theoretical investigation of two-leg ladder models is motivated not only from the academic point of view, but also from the experimental viewpoint, because the two-leg ladder motif captures the magnetic structure of a certain class of real quasi-one-dimensional magnetic materials. The most widespread family of two-leg ladder compounds form cuprates, in which one finds both experimental representatives with the dominating intra-rung interaction like SrCu_2O_3 [42, 43], $\text{Cu}_2(\text{C}_5\text{H}_{12}\text{N}_2)_2\text{Cl}_4$ [44–47], $(\text{C}_5\text{H}_{12}\text{N})_2\text{CuBr}_4$ [48], $(5\text{IAP})_2\text{CuBr}_4$ [49] as well as, the magnetic compounds with the dominating intra-leg interaction such as KCuCl_3 [50, 51], TlCuCl_3 [52–54], NH_4CuCl_3 , KCuBr_3 . Understanding the low-temperature magnetism of two-leg ladder models also turns out to be crucial for an explanation of the mechanism, which is responsible for the high-temperature superconductivity of cuprates [55]. Besides the cuprates, another experimental representatives of the two-leg ladder compounds represent vanadates $(\text{VO})_2\text{P}_2\text{O}_7$ [56], CaV_2O_5 and MgV_2O_5 [57], as well as, the polyradical BIP-BNO [58, 59].

The outline of the paper is as follows. In section 2 the model is defined and the pseudospin representation is considered. The ground-state properties of the model with and without external field are studied in section 3. The most important findings are summarized in section 4.

2. Heisenberg-Ising two-leg ladder

Let us define the spin- $\frac{1}{2}$ Heisenberg-Ising ladder through the following Hamiltonian:

$$H = \sum_{i=1}^N \left[J_1(\mathbf{s}_{1,i} \cdot \mathbf{s}_{2,i})_{\Delta} + J_2(s_{1,i}^z s_{1,i+1}^z + s_{2,i}^z s_{2,i+1}^z) + J_3(s_{2,i}^z s_{1,i+1}^z + s_{1,i}^z s_{2,i+1}^z) - h(s_{1,i}^z + s_{2,i}^z) \right], \quad (1)$$

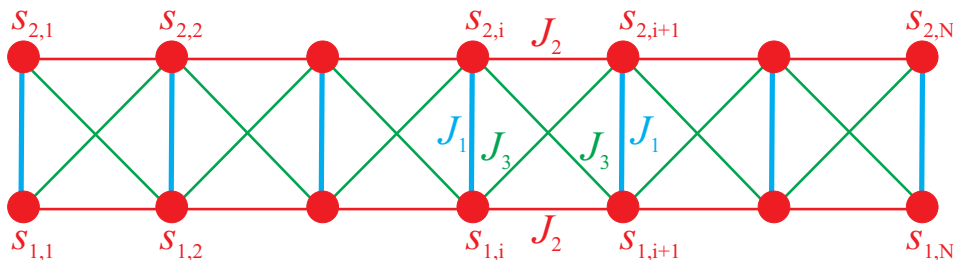


Figure 1. Quantum spin- $\frac{1}{2}$ Heisenberg-Ising two-leg ladder. Thick (thin) lines denote the Heisenberg (Ising) bonds.

where $(\mathbf{s}_{1,i} \cdot \mathbf{s}_{2,i})_\Delta = s_{1,i}^x s_{2,i}^x + s_{1,i}^y s_{2,i}^y + \Delta s_{1,i}^z s_{2,i}^z$, $s_{l,i}^\alpha$ are three spatial projections of spin- $\frac{1}{2}$ operator, the first index denotes the number of leg, the second enumerates the site, J_1 is the XXZ Heisenberg intra-rung interaction between nearest-neighbour spins from the same rung, J_2 is the Ising intra-leg interaction between nearest-neighbour spins from the same leg, J_3 is the crossing (diagonal) Ising inter-rung interaction between next-nearest-neighbour spins from different rungs, h is the external magnetic field. We also imply the periodic boundary conditions $\mathbf{s}_{1,N+1} \equiv \mathbf{s}_{1,1}$ and $\mathbf{s}_{2,N+1} \equiv \mathbf{s}_{2,1}$ along legs. The coupling constants J_2 and J_3 can be interchanged by renumbering of the sites, as well as their signs can be simultaneously reverted by spin rotations. Therefore, the Hamiltonians $H(J_2, J_3)$, $H(J_3, J_2)$ and $H(-J_2, -J_3)$ in zero field have equal eigenvalues and the corresponding models are thermodynamically equivalent.

It can be checked that z -projection of total spin on a rung $S_i^z = s_{1,i}^z + s_{2,i}^z$ commutes with the total Hamiltonian $[S_i^z, H] = 0$ and hence, it represents a conserved quantity. For further convenience, it is therefore advisable to take advantage of the bond representation, which has been originally suggested by Lieb, Schultz and Mattis for the Heisenberg-Ising chain [13]. Let us introduce the bond-state basis consisting of four state vectors:

$$\begin{aligned} |\phi_{0,0}^i\rangle &= \frac{1}{\sqrt{2}}(|\downarrow_{1,i}\uparrow_{2,i}\rangle - |\uparrow_{1,i}\downarrow_{2,i}\rangle), & |\phi_{1,0}^i\rangle &= \frac{1}{\sqrt{2}}(|\downarrow_{1,i}\uparrow_{2,i}\rangle + |\uparrow_{1,i}\downarrow_{2,i}\rangle), \\ |\phi_{1,-}^i\rangle &= \frac{1}{\sqrt{2}}(|\uparrow_{1,i}\uparrow_{2,i}\rangle - |\downarrow_{1,i}\downarrow_{2,i}\rangle), & |\phi_{1,+}^i\rangle &= \frac{1}{\sqrt{2}}(|\uparrow_{1,i}\uparrow_{2,i}\rangle + |\downarrow_{1,i}\downarrow_{2,i}\rangle). \end{aligned} \quad (2)$$

These states are the eigenstates of the Heisenberg coupling between two spins located on the i th rung, i.e. $|\phi_{0,0}^i\rangle$ is the singlet-bond state, $|\phi_{1,0}^i\rangle$, $|\phi_{1,\pm}^i\rangle$ are triplet states. Following [13] two subspaces can be singled out in the bond space: i) $|\phi_{0,0}^i\rangle$, $|\phi_{1,0}^i\rangle$ and ii) $|\phi_{1,+}^i\rangle$, $|\phi_{1,-}^i\rangle$. The first and second subspaces corresponds to $(S_i^z)^2 = 0$ and $(S_i^z)^2 = 1$ respectively, and the Hamiltonian can be diagonalized separately in each subspace. We can introduce the index of subspace at i -th site: $n_i = 0(1)$ if the given state is in the subspace with $(S_i^z)^2 = 0$ ($(S_i^z)^2 = 1$) spanned by states $|\phi_{0,0}^i\rangle$, $|\phi_{1,0}^i\rangle$ ($|\phi_{1,-}^i\rangle$, $|\phi_{1,+}^i\rangle$). According to [13], let us also call the bond states as purity (impurity) states if $n_i = 0(1)$. If one makes pseudospin notations for the states $|\phi_{0,0}^i\rangle = |\downarrow\rangle_0^i$, $|\phi_{1,0}^i\rangle = |\uparrow\rangle_0^i$, the action of the spin- $\frac{1}{2}$ operators in the subspace $n_i = 0$ can be expressed in terms of new raising and lowering operators:

$$\begin{aligned} s_{1,i}^z &= -\frac{1}{2}(a_i^+ + a_i) = -\tilde{s}_i^x, & s_{2,i}^z &= \frac{1}{2}(a_i^+ + a_i) = \tilde{s}_i^x, \\ (\mathbf{s}_{1,i} \cdot \mathbf{s}_{2,i})_\Delta &= a_i^+ a_i - \frac{2 + \Delta}{4} = \tilde{s}_i^z - \frac{\Delta}{4}. \end{aligned} \quad (3)$$

The operators a_i^+ , a_j satisfy the Pauli algebra ($\{a_i, a_i^+\} = 0$, $\{a_i, a_j\} = \{a_i^+, a_j^+\} = 0$, $[a_i, a_j] = [a_i, a_j^+] = [a_i^+, a_j^+] = 0$ for $i \neq j$), and half of their sum can be identified as a new pseudospin operator \tilde{s}_i^x .

Analogously, one can consider the pseudospin representation of the subspace $n_i = 1$ ($|\phi_{1,-}^i\rangle = |\downarrow\rangle_1^i$, $|\phi_{1,+}^i\rangle = |\uparrow\rangle_1^i$) and find the action of spin operators in it as follows:

$$s_{1,i}^z = \frac{1}{2}(a_i^+ + a_i) = \tilde{s}_i^x, \quad s_{2,i}^z = \frac{1}{2}(a_i^+ + a_i) = \tilde{s}_i^x, \quad (\mathbf{s}_{1,i} \cdot \mathbf{s}_{2,i})_\Delta = \frac{\Delta}{4}. \quad (4)$$

Combining (3), (4) we find the general expressions for the pseudospin representation of these operators, which are valid in both subspaces:

$$s_{1,i}^z = (2n_i - 1)\tilde{s}_i^x, \quad s_{2,i}^z = \tilde{s}_i^x, \quad (\mathbf{s}_{1,i} \cdot \mathbf{s}_{2,i})_\Delta = (1 - n_i)\tilde{s}_i^z + \frac{\Delta}{4}(2n_i - 1). \quad (5)$$

The effective Hamiltonian can be rewritten in terms of new operators as follows:

$$H = \sum_{i=1}^N \left\{ J_1(1 - n_i)\tilde{s}_i^z - 2hn_i\tilde{s}_i^x + \frac{J_1\Delta}{4}(2n_i - 1) + [4J_2n_in_{i+1} - 2(J_2 - J_3)(n_i + n_{i+1} - 1)]\tilde{s}_i^x\tilde{s}_{i+1}^x \right\}. \quad (6)$$

It is noteworthy that equation (5) can be considered as some nonlinear spin transformation from $s_{1,i}^\alpha, s_{2,i}^\alpha$ to new operators $s'_{1,i}^\alpha, s'_{2,i}^\alpha$, where e.g. $s'_{1,i}^z = (n_i - \frac{1}{2})$, $s'_{2,i}^\alpha = \tilde{s}_i^\alpha$. The transformation can be generated by the following unitary operator:

$$U = \prod_{i=1}^N \exp \left[-i\frac{\pi}{2}(s_{1,i}^x + s_{2,i}^x) \right] \exp \left(i\pi s_{1,i}^x s_{2,i}^x \right) \exp \left(-i\frac{\pi}{2}s_{2,i}^y \right) \exp \left(i\pi s_{2,i}^z \right). \quad (7)$$

The crucial point is the second factor, which introduces the nonlinearity. Other terms are the rotation in spin space, they are used to adjust the transformed operators to the form of (5). Finally, the spin operators are transformed as follows:

$$\begin{aligned} U s_{1,i}^x U^+ &= s_{1,i}^x, & U s_{1,i}^y U^+ &= 2s_{1,i}^y s_{2,i}^x, & U s_{1,i}^z U^+ &= 2s_{1,i}^z s_{2,i}^x, \\ U s_{2,i}^x U^+ &= 2s_{1,i}^x s_{2,i}^z, & U s_{2,i}^y U^+ &= -2s_{1,i}^x s_{2,i}^y, & U s_{2,i}^z U^+ &= s_{2,i}^x. \end{aligned} \quad (8)$$

The transformed Hamiltonian has the form of the quantum Ising chain with composite spins in an effective longitudinal and transverse magnetic field:

$$\begin{aligned} UHU^+ &= \sum_{i=1}^N \left\{ \frac{J_1}{2} (1 - 2s_{1,i}^z) s_{2,i}^z + \frac{J_1\Delta}{2} s_{1,i}^z + [J_2(4s_{1,i}^z s_{1,i+1}^z + 1) \right. \\ &\quad \left. + 2J_3(s_{1,i+1}^z + s_{1,i}^z)] s_{2,i}^x s_{2,i+1}^x - h(1 + 2s_{1,i}^z) s_{2,i}^x \right\}. \end{aligned} \quad (9)$$

The straightforward correspondence $s_{1,i}^z = n_i - \frac{1}{2}$, $s_{2,i}^\alpha = \tilde{s}_i^\alpha$ leads to the equivalence between the Hamiltonians (6) and (9). It should be noted that such kind of a representation remains valid also in case of the asymmetric ladder having both diagonal (crossing) Ising interactions different from each other.

3. Ground state of the Heisenberg-Ising two-leg ladder

The Hamiltonian (6) can also be rewritten in the following more symmetric form:

$$\begin{aligned} H &= \sum_{i=1}^N \left\{ J_1(1 - n_i)\tilde{s}_i^z - 2hn_i\tilde{s}_i^x + \frac{J_1\Delta}{4}(2n_i - 1) \right. \\ &\quad \left. + [2(J_2 + J_3)n_in_{i+1} + 2(J_2 - J_3)(1 - n_i)(1 - n_{i+1})]\tilde{s}_i^x\tilde{s}_{i+1}^x \right\}. \end{aligned} \quad (10)$$

This form serves in evidence that the effective model splits at i th site into two independent chains provided that two neighbouring bonds are being in different

subspaces, i.e. $n_i \neq n_{i+1}$. The uniform Hamiltonians, when all $n_i = 0$ or all $n_i = 1$, read:

$$H^0 = \sum_{i=1}^N \left[J_1 \left(\tilde{s}_i^z - \frac{\Delta}{4} \right) + 2(J_2 - J_3) \tilde{s}_i^x \tilde{s}_{i+1}^x \right], \quad (11)$$

$$H^1 = \sum_{i=1}^N \left[2(J_2 + J_3) \tilde{s}_i^x \tilde{s}_{i+1}^x - 2h \tilde{s}_i^x + \frac{J_1 \Delta}{4} \right]. \quad (12)$$

If all bonds are in purity states ($n_i = 0$), one obtains the effective Hamiltonian of the Ising chain in the transverse field that is exactly solvable within Jordan-Wigner fermionization [60, 61]. If all bonds are in impurity states ($n_i = 1$), one comes to the Ising chain in the longitudinal field that is solvable by the transfer-matrix method (see e.g. [62]). Accordingly, the ground-state energy of the model in $n_i = 0$ subspace is given by [61]:

$$e_0^0 = \lim_{N \rightarrow \infty} \frac{E_0^0(N)}{N} = -\frac{(J_1 + |J_2 - J_3|)}{\pi} \mathbf{E}(\sqrt{1 - \gamma^2}) - \frac{J_1 \Delta}{4}, \quad (13)$$

where $\gamma = \frac{J_1 - |J_2 - J_3|}{J_1 + |J_2 - J_3|}$ and $\mathbf{E}(\kappa) = \int_0^{\frac{\pi}{2}} d\theta \sqrt{1 - \kappa^2 \sin^2 \theta}$ is the complete elliptic integral of the second kind.

The ground-state energy of the model in $n_i = 1$ subspace is given by the ground-state energy of the effective Ising chain in the longitudinal field:

$$e_0^1 = \lim_{N \rightarrow \infty} \frac{E_0^1(N)}{N} = \begin{cases} \frac{J_1 \Delta}{4} + \frac{J_2 + J_3}{2} - |h|, & \text{if } |h| > (J_2 + J_3), \\ \frac{J_1 \Delta}{4} - \frac{J_2 + J_3}{2}, & \text{if } |h| \leq (J_2 + J_3). \end{cases} \quad (14)$$

The upper (lower) case corresponds to the ferromagnetically (antiferromagnetically) ordered state being the ground state at strong (weak) enough magnetic fields.

3.1. Ground-state phase diagram in a zero field

If the external field vanishes ($h = 0$), it is sufficient to show that the inequality $E_0^0(N_1) + E_0^0(N_2) \geq E_0^0(N_1 + N_2)$ holds for any finite transverse Ising chain with free ends in order to prove that the ground state always corresponds to a uniform bond configuration. Here $E_0^0(N)$ denotes the ground state energy of the Hamiltonian:

$$H^0(N) = 2(J_2 - J_3) \sum_{i=1}^{N-1} \tilde{s}_i^x \tilde{s}_{i+1}^x + J_1 \sum_{i=1}^N \left(\tilde{s}_i^z - \frac{\Delta}{4} \right). \quad (15)$$

Indeed, two independent chains of size N_1 and N_2 can be represented by the following Hamiltonian:

$$\begin{aligned} H^0(N_1, N_2) &= 2(J_2 - J_3) \sum_{i=1}^{N_1-1} \tilde{s}_i^x \tilde{s}_{i+1}^x + 2(J_2 - J_3) \sum_{i=N_1+1}^{N_1+N_2-1} \tilde{s}_i^x \tilde{s}_{i+1}^x + J_1 \sum_{i=1}^{N_1+N_2} \left(\tilde{s}_i^z - \frac{\Delta}{4} \right) \\ &= H^0(N_1 + N_2) - 2(J_2 - J_3) \tilde{s}_{N_1}^x \tilde{s}_{N_1+1}^x. \end{aligned} \quad (16)$$

If $E_0^0(N)$ and $|\psi_0^N\rangle$ are the lowest eigenvalue and eigenstate of $H^0(N)$, then $E_0^0(N_1, N_2) = E_0^0(N_1) + E_0^0(N_2)$ and $|\psi_0^{N_1, N_2}\rangle = |\psi_0^{N_1}\rangle |\psi_0^{N_2}\rangle$ are the lowest eigenvalue and eigenstate of

$H^0(N_1, N_2)$. Now, it is straightforward to show that

$$E_0^0(N_1) + E_0^0(N_2) = \langle \psi_0^{N_1, N_2} | H^0(N_1 + N_2) | \psi_0^{N_1, N_2} \rangle - 2(J_2 - J_3) \langle \psi_0^{N_1} | \tilde{s}_{N_1}^x | \psi_0^{N_1} \rangle \langle \psi_0^{N_2} | \tilde{s}_{N_1+1}^x | \psi_0^{N_2} \rangle \geq E_0^0(N_1 + N_2). \quad (17)$$

Here, we have used that $\langle \psi_0^{N_1} | \tilde{s}_{N_1}^x | \psi_0^{N_1} \rangle = 0$ for any finite chain [13, 61], and that the lowest mean value of the operator $H^0(N_1 + N_2)$ is achieved in its ground state.

It is easy to show by straightforward calculation that the same property is valid for the Ising chain with free ends in zero longitudinal field, i.e.

$$E_0^1(N_1 + N_2) = E_0^1(N_1) + E_0^1(N_2) + \frac{|J_2 + J_3|}{2} \leq E_0^1(N_1) + E_0^1(N_2). \quad (18)$$

Now, let us prove that the ground state of the whole model may correspond only to one of uniform bond configurations. It can be readily understood from (10) that the effective Hamiltonian does not contain an interaction between spins from two neighbouring bonds if they are in different subspaces [63]. It means that the effective model splits into two independent parts at each boundary ('domain wall') between the purity and impurity states. Thus, the Heisenberg-Ising ladder for any given configuration of bonds can be considered as a set of independent chains of two kinds and of different sizes. Then, the ground-state energy of any randomly chosen bond configuration will be as follows:

$$E = E_0^0(N_1) + E_0^0(N_2) + \dots + E_0^1(M_1) + E_0^1(M_2) + \dots \geq E_0^0(N_1 + N_2 + \dots) + E_0^1(M_1 + M_2 + \dots) \quad (19)$$

It is quite evident from equations (17) and (18) that the one uniform configuration, which corresponds to the state with lower energy than the other one, must be according to inequality (19) the lowest-energy state (i.e. ground state). Therefore, the model may show in the ground state the first-order quantum phase transition when the lowest eigenenergies in both subspaces becomes equal $e_0^1 = e_0^0$. Besides, there also may appear the more striking second-order (continuous) quantum phase transition at $|J_1| = |J_2 - J_3|$ in the ground state, which is inherent to the pure quantum spin chain [61]. From this perspective, the Heisenberg-Ising ladder can show a variety of quantum phase transitions in its phase diagram.

The ground-state phase diagram of the spin- $\frac{1}{2}$ Heisenberg-Ising ladder in a zero magnetic field is shown in figure 2. It reflects the symmetry of the model, i.e. it is invariant under the exchange of the Ising interactions J_2 and J_3 , as well as, under the simultaneous change of the signs of J_2 and J_3 . Altogether, five different ground states can be recognised in figure 2:

- (i) **Quantum paramagnetic (QPM) state** for $e_0^0 < e_0^1$, and $|J_1| > |J_2 - J_3|$: the equivalent transverse Ising chain (11) is in the gapped disordered state with no spontaneous magnetization $\langle \tilde{s}_i^x \rangle = 0$ and non-zero magnetization $\langle \tilde{s}_i^z \rangle \neq 0$ induced by the effective transverse field. For the initial Heisenberg-Ising ladder it means that the rung singlet dimers are dominating on Heisenberg bonds in the ground state. Although each bond may possess the antiferromagnetic order, the interaction along legs demolishes it and leads to the disordered quantum paramagnetic state.

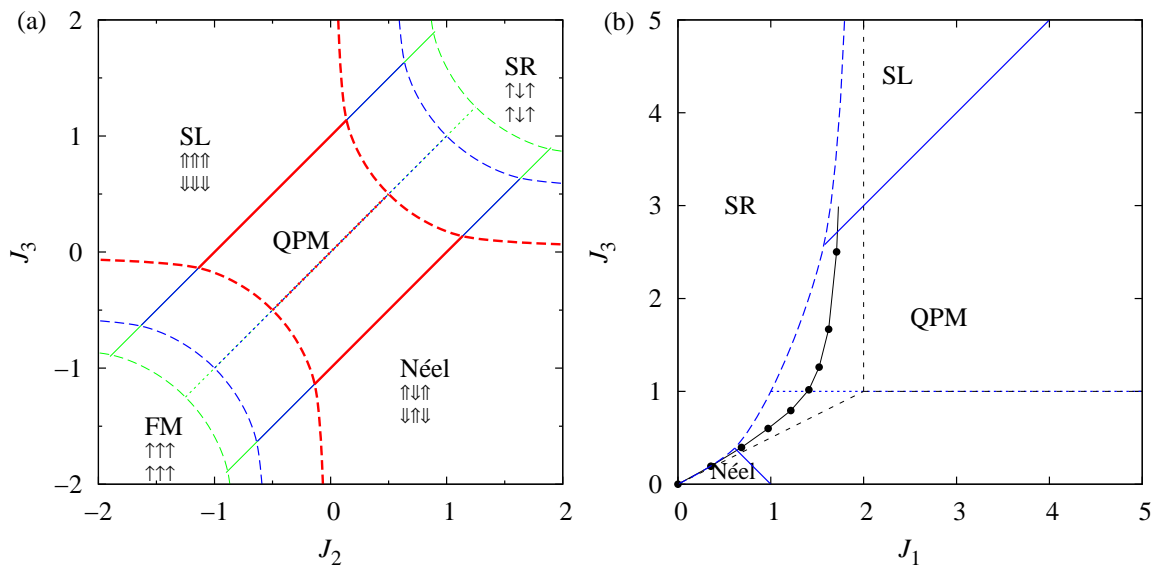


Figure 2. Ground-state phase diagrams for the spin- $\frac{1}{2}$ Heisenberg-Ising two-leg ladder in an absence of the external magnetic field ($h = 0$). Broken (solid) lines denote the lines of first-order (second-order) quantum phase transitions, dotted lines denote the rung singlet-dimer state.

(a) $J_1 = 1$, $\Delta = 0.0$ (red), 1.0(blue), 1.5(green) (from thick to thin lines);

(b) $J_2 = 1$, $\Delta = 1$. Thick solid and broken (blue) lines are the ground-state boundaries of the Heisenberg-Ising ladder, the thin line with dots shows the ground-state boundary of the Heisenberg ladder [26] and straight broken lines the ground-state boundaries of the Ising ladder.

- (ii) **Stripe Leg (SL) state** for $e_0^0 < e_0^1$, and $|J_1| < J_3 - J_2$: the equivalent transverse Ising chain exhibits the spontaneous ferromagnetic ordering with $\langle \tilde{s}_i^x \rangle \neq 0$. Due to relations (3) and (4), one obtains for the Heisenberg-Ising ladder $\langle s_{1,i}^z \rangle = \langle s_{1,i+1}^z \rangle = -\langle s_{2,i}^z \rangle = -\langle s_{2,i+1}^z \rangle \neq 0$. This result is taken to mean that the Heisenberg-Ising ladder shows a ferromagnetic order along legs and antiferromagnetic order along rungs, i.e. the magnetizations of chains are opposite. The staggered magnetization as the relevant order parameter in this phase is non-zero and it exhibits evident quantum reduction of the magnetization given by: $m_{SL}^z = \frac{1}{2N} \sum_{i=1}^N (\langle s_{1,i}^z \rangle - \langle s_{2,i}^z \rangle) = \frac{1}{2} [1 - J_1^2 / (J_2 - J_3)^2]^{\frac{1}{8}}$. Here we used the result for the spontaneous magnetization of transverse Ising chain [61].
- (iii) **Néel state** for $e_0^0 < e_0^1$, and $|J_1| < J_2 - J_3$: the effective transverse Ising chain shows the spontaneous antiferromagnetic order with $\langle \tilde{s}_i^x \rangle = (-1)^i m_x \neq 0$. For the Heisenberg-Ising ladder one consequently obtains $\langle s_{1,i}^z \rangle = -\langle s_{1,i+1}^z \rangle = -\langle s_{2,i}^z \rangle = \langle s_{2,i+1}^z \rangle \neq 0$. Hence, it follows that the nearest-neighbour spins both along legs as well as rungs exhibit predominantly antiferromagnetic ordering. The dependence of staggered magnetization as the relevant order parameter is quite analogous to the previous case $m_{AF}^z = \frac{1}{2N} \sum_{i=1}^N (-1)^i (\langle s_{1,i}^z \rangle - \langle s_{2,i}^z \rangle) = \frac{1}{2} [1 - J_1^2 / (J_2 - J_3)^2]^{\frac{1}{8}}$.
- (iv) **Stripe Rung (SR) state** for $e_0^1 < e_0^0$, $J_2 > 0$, $J_3 > 0$: the model shows classical

ordering in this phase with the antiferromagnetically ordered nearest-neighbour spins along legs and the ferromagnetically ordered nearest-neighbour spins along rungs.

- (v) **Ferromagnetic (FM) state** for $e_0^1 < e_0^0$, $J_2 < 0$, $J_3 < 0$: the ground state corresponds to the ideal fully polarized ferromagnetic spin state.

The results displayed in figure 2(a) demonstrate that the Heisenberg-Ising ladder is in the disordered QPM phase whenever a relative strength of both Ising interactions J_2 and J_3 is sufficiently small compared to the Heisenberg intra-rung interaction J_1 . It is noteworthy, moreover, that the QPM phase reduces to a set of fully non-correlated singlet dimers placed on all rungs (the so-called rung singlet-dimer state) along the special line $J_2 = J_3$ up to $e_0^0 < e_0^1$, which is depicted in figure 2 by dotted lines. Under this special condition, the intra-rung spin-spin correlation represents the only non-zero pair correlation function and all the other short-ranged spin-spin correlations vanish and/or change their sign across the special line $J_2 = J_3$. It should be remarked that the completely identical ground state can also be found in the symmetric Heisenberg two-leg ladder with $J_2 = J_3$ (see figure 2(b)). To compare with, the rung singlet-dimer state is being the exact ground state of the symmetric Heisenberg-Ising ladder with $\Delta = 1$ for $J_1 > J_2$, while the symmetric Heisenberg ladder displays this simple factorizable ground state for $J_1 > 1.4015J_2$ [35, 36] (this horizontal line is for clarity not shown in figure 2(b) as it exactly coincides with the ground-state boundary of the Heisenberg-Ising ladder extended over larger parameter space). It should be stressed, however, that the short-range spin-spin correlations become non-zero in QPM whenever $J_2 \neq J_3$ even if this phase still preserves its disordered nature with the prevailing character of the rung singlet-dimer state. To support this statement, the zero-temperature dependencies of the order parameters and the nearest-neighbour spin-spin correlation along legs are plotted in figure 3. The relevant order parameters evidently disappear in QPM, whereas the nearest-neighbour correlation function changes its sign when passing through the special line $J_2 = J_3$ of the rung singlet-dimer state.

Note furthermore that the Heisenberg-Ising ladder undergoes the second-order quantum phase transition from the disordered QPM phase to the spontaneously long-range ordered Néel or SL phase, which predominantly appear in the parameter region where one from both Ising couplings J_2 and J_3 is being antiferromagnetic and the other one is ferromagnetic. The significant quantum reduction of staggered order parameters implies an obvious quantum character of both Néel as well as SL phases in which the antiferromagnetic correlation on rungs still dominates (see figure 3). Thus, the main difference between both the quantum long-range ordered phases emerges in the character nearest-neighbour correlation along legs, which is ferromagnetic in the SL phase but antiferromagnetic in the Néel phase. The continuous vanishing of the order parameters depicted in figure 3(a) provides a direct evidence of the second-order quantum phase transition between the disordered QPM phase and the ordered SL (or Néel) phase, which is also accompanied with the weak-singular behaviour of the nearest-neighbour

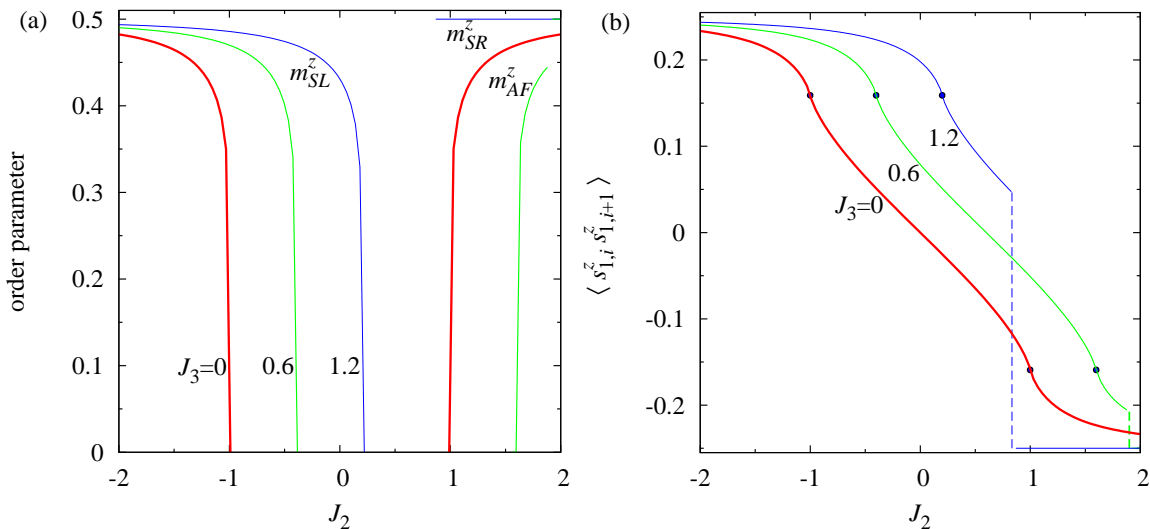


Figure 3. Zero-temperature variations of: (a) the order parameters; (b) the nearest-neighbour spin-spin correlation along legs; as a function of the Ising intra-leg interaction J_2 for $J_1 = 1$, $\Delta = 1$ and three different values of the crossing Ising interaction $J_3 = 0, 0.6, 1.2$.

correlation function visualized in figure 3(b) by black dots. Here it should be noted that the zz correlation function of the Heisenberg-Ising ladder can be easily derived from the result of the xx correlation function of the transverse Ising chain calculated in [61]. Last but not least, the strong enough Ising interactions J_2 and J_3 may break the antiferromagnetic correlation along rungs and lead to a presence of the fully ordered ferromagnetic rung states FM or SR depending on whether both Ising interactions are ferromagnetic or antiferromagnetic, respectively. It should be noticed that this change is accompanied with a discontinuous (first-order) quantum phase transition on behalf of a classical character of both FM and SR phases, which can be also clearly seen in figure 3 from an abrupt change of the order parameters as well as the nearest-neighbour correlation function.

Finally, let us also provide a more detailed comparison between the ground-state phase diagrams of the Heisenberg, Heisenberg-Ising and Ising two-leg ladders all depicted in figure 2(b). One can notice that the displayed ground-state phase diagrams of the Heisenberg and Heisenberg-Ising two-leg ladders have several similar features. The phase boundary between the classically ordered SR phase and three quantum phases (QPM, SL, Néel) of the Heisenberg-Ising ladder follows quite closely the first-order phase boundary between the Haldane-type phase and the dimerized phase of the pure Heisenberg ladder obtained using the series expansion and exact diagonalization [26]. Of course, the most fundamental difference lies in the character of SR and Haldane phases, because the former phase exhibits a classical long-range order contrary to a more spectacular topological order of the pure quantum Haldane-type phase with a non-zero string order parameter [31] even though the ferromagnetic

intra-rung correlation is common for both phases. The difference between the ground states of the Heisenberg-Ising and pure Heisenberg two-leg ladder becomes much less pronounced in the parameter region with the strong intra-rung interaction J_1 , which evokes the quantum phases in the ground state of both these models. In the case of a sufficiently strong frustration $J_2 \sim J_3$, the ground state of the Heisenberg-Ising ladder forms the disordered QPM phase, whereas the antiferromagnetic or ferromagnetic (Néel or SL) long-range order emerges along the legs if the diagonal coupling J_3 is much weaker or stronger than the intra-leg interaction J_2 . Note that the quantum Néel and SL phases have several common features (e.g. predominant antiferromagnetic correlations along rungs) with the disordered QPM phase from which they evolve when crossing continuous quantum phase transitions given by the set of equations: $J_3 = J_2 - J_1$ (for $J_3 < J_2$) and $J_3 = J_2 + J_1$ (for $J_3 > J_2$). It cannot be definitely ruled out whether or not these quantum ordered phases may become the ground state of the pure Heisenberg ladder, because they are also predicted by the bond-mean-field approximation [39–41] but have not been found by the most of the numerical methods. Further numerical investigations of the Heisenberg ladder are therefore needed to clarify this unresolved issue.

3.2. Ground-state phase diagram in a non-zero field

When the external field h is switched on, the inequality for the ground states of the Ising chain in the longitudinal field (18) is generally valid only for $J_1 + J_2 \leq 0$ or $J_1 + J_2 \geq 2|h|$. Hence, it is necessary to modify the procedure of finding the ground states inside the region where the relation (18) is broken. However, one may use with a success the method suggested by Shastry and Sutherland [25,64] in order to find the ground states inside this parameter region. Let us represent our effective Hamiltonian (10) in the form:

$$\begin{aligned}
 H &= \sum_{i=1}^N H_{i,i+1}, \\
 H_{i,i+1} &= \frac{1}{2} \sum_{l=i}^{i+1} \left\{ J_1(1 - n_l) \tilde{s}_l^z - 2hn_l \tilde{s}_l^x + \frac{J_1 \Delta}{4} (2n_l - 1) \right\} \\
 &\quad + [2(J_2 + J_3)n_i n_{i+1} + 2(J_2 - J_3)(1 - n_i)(1 - n_{i+1})] \tilde{s}_i^x \tilde{s}_{i+1}^x. \tag{20}
 \end{aligned}$$

Then, one can employ the variational principle implying that $E_0 \geq \sum_{l=1}^N E_0(l, l+1)$, where $E_0(l, l+1)$ is the lowest eigenenergy of $H_{l,l+1}$.

Looking for the eigenenergies of $H_{l,l+1}$ it is enough to find the lowest eigenstate of each bond configuration:

- $n_i = n_{i+1} = 0$, $E_0^{0,0}(i, i+1) = -\frac{1}{2} \sqrt{J_1^2 + (J_2 - J_3)^2} - \frac{J_1 \Delta}{4}$;
- $n_i = n_{i+1} = 1$,

$$E_0^{1,1}(i, i+1) = \begin{cases} \frac{J_1 \Delta}{4} + \frac{J_2 + J_3}{2} - |h|, & \text{if } |h| > (J_2 + J_3) \text{ (FM)}, \\ \frac{J_1 \Delta}{4} - \frac{J_2 + J_3}{2}, & \text{if } |h| \leq (J_2 + J_3) \text{ (AF)}. \end{cases}$$

- $n_i = 0, n_{i+1} = 1$ ($n_i = 1, n_{i+1} = 0$), $E_0^{0,1}(i, i+1) = E_0^{1,0}(i, i+1) = -\frac{J_1}{4} - \frac{|h|}{2}$.

The phase corresponding to the alternating bond configuration $n_i = 0, n_{i+1} = 1$ will be hereafter referred to as the staggered bond (SB) phase. It should be mentioned that there does not exist in the SB phase any correlations between spins from different rungs and the overall energy comes from the intra-rung spin-spin interactions and the Zeeman's energy of the fully polarized rungs [63]. It can be easily seen from a comparison of $E_0^{0,1}(i, i+1)$ and $E_0^{1,1}(i, i+1)$ that the eigenenergy of the SB phase $E_0^{0,1}(i, i+1)$ has always lower energy than the lowest eigenenergy of the fully polarized state $E_0^{1,1}(i, i+1)$ inside the stripe:

$$J_2 + J_3 - \frac{J_1(1 + \Delta)}{2} \leq |h| \leq J_2 + J_3 + \frac{J_1(1 + \Delta)}{2}. \quad (21)$$

Note that the ferromagnetic ordering is preferred for external fields above this stripe $|h| \geq J_2 + J_3 + \frac{J_1(1+\Delta)}{2}$, while the antiferromagnetic ordering becomes the lowest-energy state below this stripe $|h| \leq J_2 + J_3 - \frac{J_1(1+\Delta)}{2}$.

If one compares the respective eigenenergies of the staggered bond phase $E_0^{0,1}(i, i+1)$ and the uniform purity phase $E_0^{0,0}(i, i+1)$ ($n_i = n_{i+1} = 0$), one gets another condition implying that $E_0^{0,1}(i, i+1)$ becomes lower than $E_0^{0,0}(i, i+1)$ only if:

$$|h| \geq \sqrt{J_1^2 + (J_2 - J_3)^2} - \frac{J_1(1 - \Delta)}{2}. \quad (22)$$

This means that the SB phase with the overall energy $E_0^{0,1} = -N(J_1 + 2|h|)/4$ becomes the ground state inside the region confined by conditions (21) and (22). The lowest field, which makes the SB phase favourable, can be also found as:

$$|h_{min}| = \frac{J_1(1 + \Delta)}{2}. \quad (23)$$

Similarly, one may also find the condition under which two eigenenergies corresponding to the uniform impurity configuration $E_0^{1,1}(n_i = n_{i+1} = 1)$ become lower than the respective eigenenergy of the uniform purity configuration $E_0^{0,0}(n_i = n_{i+1} = 0)$. The ferromagnetic state of the uniform impurity configuration becomes lower if the external field exceeds the boundary value:

$$|h| \geq \frac{1}{2} \left[J_2 + J_3 + J_1\Delta + \sqrt{J_1^2 + (J_2 - J_3)^2} \right], \quad (24)$$

whereas the condition for the antiferromagnetic state of the uniform impurity configuration is independent of the external field:

$$J_1\Delta + \sqrt{J_1^2 + (J_2 - J_3)^2} \leq (J_2 + J_3). \quad (25)$$

It is worthy of notice that it is not possible to find the ground state outside the boundaries (22), (24), (25) using the variational principle. However, it is shown in the appendix that the bond configuration, which corresponds to the ground state, cannot exceed period two. Therefore, one has to search for the ground state just among the states that correspond to the following bond configurations: all $n_i = 0$; all $n_i = 1$; $n_{2i-1} = 0, n_{2i} = 1$ ($n_{2i-1} = 1, n_{2i} = 0$). In this respect, two phases are possible inside

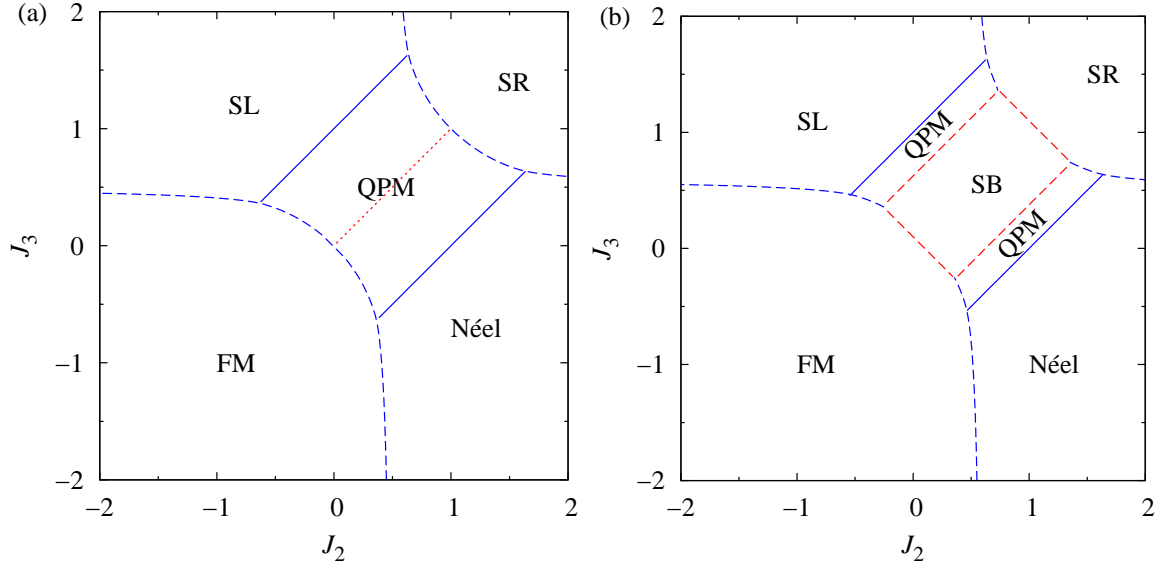


Figure 4. Ground-state phase diagrams for the Heisenberg-Ising two-leg ladder in the $J_2 - J_3$ plane for $J_1 = 1$, $\Delta = 1$ and two different values of the external field: (a) $h = 1.0$; (b) $h = 1.1$.

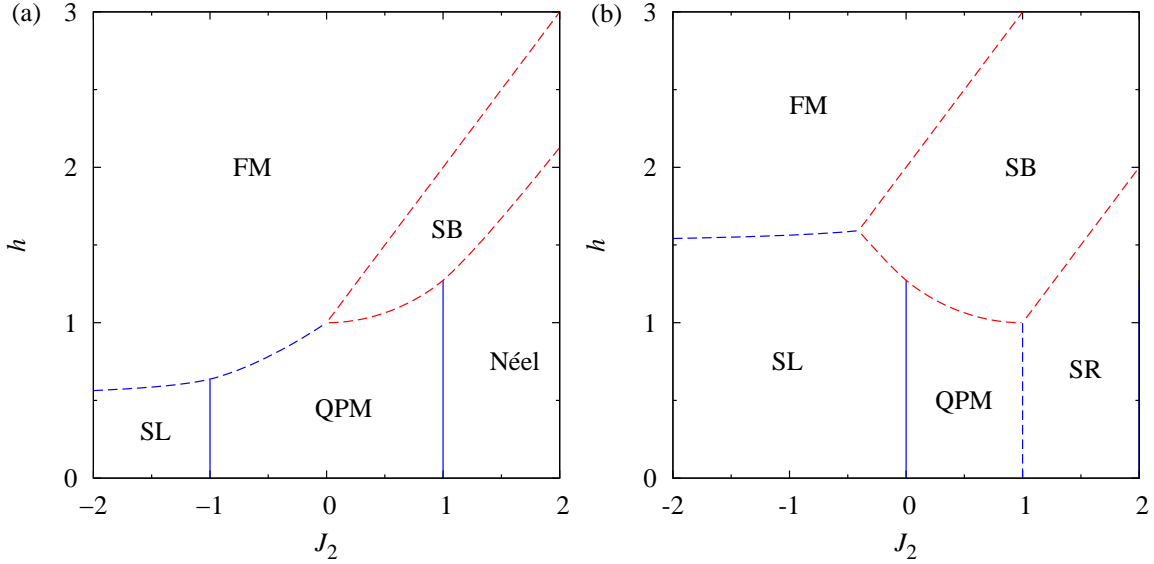


Figure 5. Ground-state phase diagrams for the Heisenberg-Ising two-leg ladder in the $J_2 - h$ plane for $J_1 = 1$, $\Delta = 1$ and two different values of the crossing interaction: (a) $J_3 = 0$; (b) $J_3 = 1$.

the stripe given by (21). The ground state of the Heisenberg-Ising ladder forms the SB phase if $e_0^{0,1} < e_0^0$:

$$|h| \geq \frac{2(J_1 + |J_2 - J_3|)}{\pi} \mathbf{E}(\sqrt{1 - \gamma^2}) - \frac{J_1(1 - \Delta)}{2}. \quad (26)$$

Several ground-state phase diagrams are plotted in figures 4-6 for a non-zero magnetic field. The most interesting feature stemming from these phase diagrams is

that the SB phase may become the ground state for the magnetic field $h \geq \frac{J_1(1+\Delta)}{2}$, which is sufficiently strong to break the rung singlet-dimer state. It can be observed from figure 4 that the SB phase indeed evolves along the line of the rung singlet-dimer state and replaces the QPM phase in the ground-state phase diagram. The external magnetic field may thus cause an appearance of another peculiar quantum SB phase with the translationally broken symmetry, i.e. the alternating singlet and fully polarized triplet bonds on the rungs of the two-leg ladder. Hence, it follows that the SB phase emerges at moderate values of the external magnetic field and it consequently leads to a presence of the intermediate magnetization plateau at a half of the saturation magnetization. It is quite apparent from figures 5(a), 6(a) that the Heisenberg-Ising ladder without the frustrating diagonal Ising interaction $J_3 = 0$ exhibits this striking magnetization plateau just for the particular case of the antiferromagnetic Ising intra-leg interaction $J_2 > 0$. On the other hand, the fractional magnetization plateau inherent to a presence of the SB phase is substantially stabilized by the spin frustration triggered by the non-zero diagonal Ising interaction $J_3 \neq 0$ and hence, the plateau region may even extend over a relatively narrow region of the ferromagnetic Ising intra-leg interaction $J_2 < 0$ as well (see figure 5(b)).

It should be noted that the same mechanism for an appearance of the magnetization plateau has also been predicted for the spin- $\frac{1}{2}$ Heisenberg two-leg ladder by making use of exact numerical diagonalization and DMRG methods [22–25, 34]. Let us therefore conclude our study by comparing the respective ground-state phase diagrams of the Heisenberg-Ising and Heisenberg two-leg ladders in a presence of the external magnetic field displayed in figure 6. According to this plot, both models give essentially the same magnetization process in the strong-coupling limit of the Heisenberg intra-rung interaction $J_1 \gtrsim 1.5$, where two subsequent field-induced transitions in the following order QPM-SB-FM can be observed and consequently, the magnetization exhibits two abrupt jumps at the relevant transition fields. On the other hand, the fundamental differences can be detected in the relevant magnetization process of the Heisenberg-Ising and Heisenberg ladders in the weak-coupling limit of the intra-rung interaction J_1 . At low fields, the quantum Haldane-like phase constitutes the ground state of the pure Heisenberg ladder in contrast to the classical SR phase, which is being the low-field ground state of the Heisenberg-Ising ladder. In addition, the Heisenberg-Ising ladder still exhibits a magnetization plateau corresponding to a gapped SB phase at intermediate values of the magnetic field in this parameter space, while a continuous increase of the magnetization can be observed in the pure Heisenberg ladder due to a presence of the gapless Luttinger-liquid phase at moderate fields. Finally, it is also noteworthy that the saturation fields towards FM phase are also quite different for the Heisenberg-Ising and Heisenberg ladders in the weak-coupling limit of the Heisenberg intra-rung interaction.

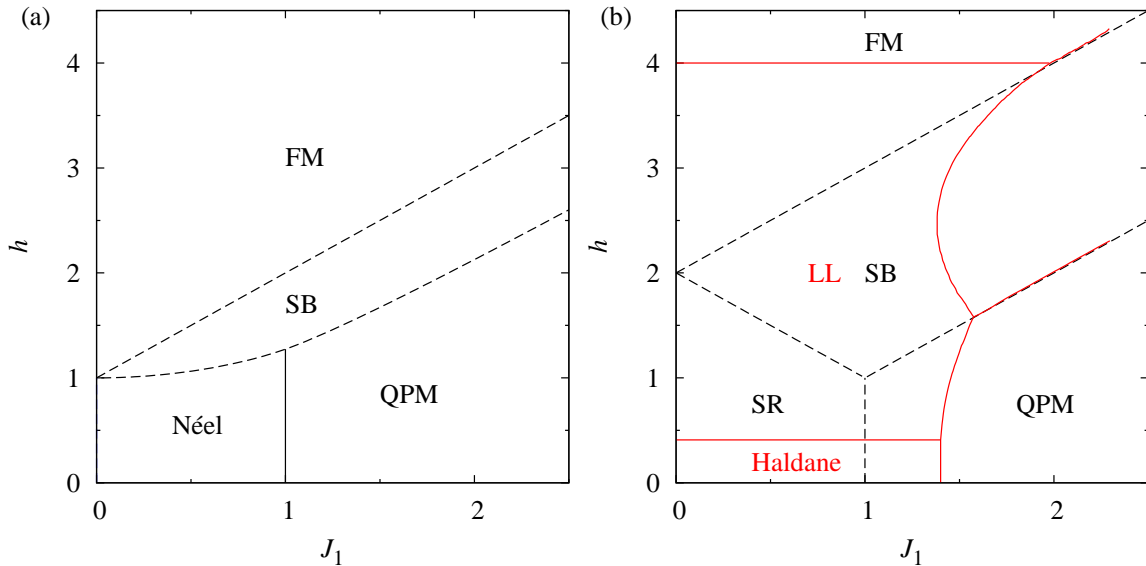


Figure 6. Ground-state phase diagram for the Heisenberg-Ising two-leg ladder in the $J_1 - h$ plane for $J_2 = 1$, $\Delta = 1$ and two different values of the crossing interaction: (a) $J_3 = 0$; (b) $J_3 = 1$. For a comparison, figure 6(b) depicts by red lines the ground-state phase diagram of the pure Heisenberg two-leg ladder adapted from [22].

4. Conclusions

The frustrated Heisenberg-Ising two-leg ladder was considered within the rigorous approach using that z -projection of total spin on a rung is a conserved quantity. By means of the pseudospin representation of bond states, we have proved the exact mapping correspondence between the investigated model and some generalized spin- $\frac{1}{2}$ quantum Ising chain with the composite spins in an effective longitudinal and transverse field. We have also found the unitary transformation which reproduces the analogous mapping between the models. While the bond-state representation has more transparent physical interpretation, the unitary transformation gives the complete relation between spin operators of both models, and it might be useful for searching quantum spin ladders which admit exact solutions.

It has been shown that the ground state of the model under investigation must correspond to a regular bond configuration not exceeding the period two. Hence, the true ground state will be the lowest eigenstate of either the transverse Ising chain, the Ising chain in the longitudinal field, or the non-interacting spin-chain model in the staggered longitudinal-transverse field.

The most interesting results to emerge from the present study are closely related to an extraordinary diversity of the constructed ground-state phase diagrams and the quantum phase transitions between different ground-state phases. In an absence of the external magnetic field, the ground-state phase diagram constitute four different ordered phases and one quantum paramagnetic phase. The disordered phase was characterized through short-range spin correlations, which indicate a dominating character of the

rung singlet-dimer state in this phase. On the other hand, the order parameters have been exactly calculated for all the four ordered phases, two of them having classical character and two purely quantum character as evidenced by the quantum reduction of the staggered magnetization in the latter two phases. Last but not least, it has been demonstrated that the external magnetic field of a moderate strength may cause an appearance of the peculiar SB phase with alternating character of singlet and triplet bonds on the rungs of two-leg ladder. This latter finding is consistent with a presence of the fractional magnetization plateau at a half of the saturation magnetization in the relevant magnetization process.

Acknowledgments

The authors are grateful to Oleg Derzhko for several useful comments and suggestions. T.V. was supported by the National Scholarship Programme of the Slovak Republic for the Support of Mobility of Students, PhD Students, University Teachers and Researchers. J.S. acknowledges the financial support under the grant VEGA 1/0234/12.

Appendix A. Ground-state bond configuration in magnetic field

In general each state of the model can be represented as an array of alternating purity and impurity non-interacting clusters of different length. One can formally write the lowest energy of some configuration as

$$E = E_0(N_1, M_1) + E_0(N_2, M_2) + \dots + E_0(N_L, M_L), \quad (\text{A.1})$$

where $E_0(N_i, M_i) = E_0^0(N_i) + E_0^1(M_i)$ is the lowest energy of the complex of two independent spin chains which correspond to the purity and impurity bond states, $N_1 + M_1 + N_2 + M_2 + \dots + N_L + M_L = N$. If $e_0(N_i, M_i) = E_0(N_i, M_i)/(N_i + M_i)$ corresponds to the lowest energy per spin among other clusters, it is evident that the ground state configuration is alternating purity and impurity clusters of length N_i and M_i .

Let us consider at first the case when h is restricted by condition (21). If the configuration contains the cluster of more than 2 impurity bonds, its energy can be lowered by adding pure bond in-between. If condition (21) is valid, such a configuration can achieve a lower energy. Using this procedure we can reduce the number of sites in impurity clusters to 2, i.e. only $E_0(N, 1)$ or $E_0(N, 2)$ can correspond to the ground state.

Define the energy per spin for each configuration as:

$$e_0(N, 1) = \frac{E_0^0(N) + E_0^1(1)}{N + 1}, \quad (\text{A.2})$$

$$e_0(N, 2) = \frac{E_0^0(N) + E_0^1(2)}{N + 2}. \quad (\text{A.3})$$

If $e_0(1, 1) < e_0(2, 1)$ and so on ($e_0(N, 1) < e_0(N + 1, 1)$) the ground state corresponds to the staggered bond configuration. Suppose that for some N

$$\Delta e_0(N - 1) = e_0(N, 1) - e_0(N - 1, 1)$$

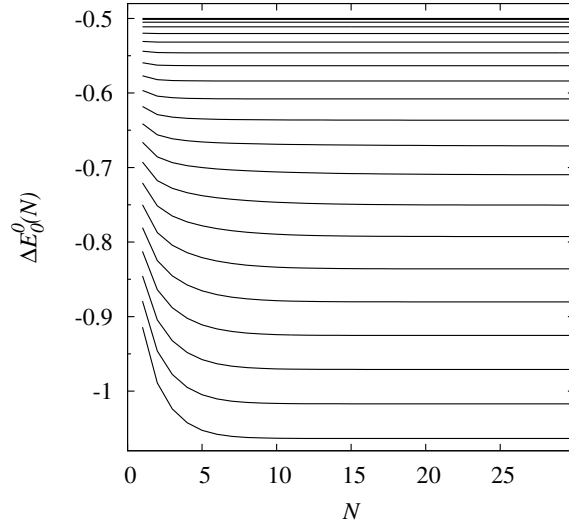


Figure A1. $\Delta E_0^0(N) = E_0^0(N+1) - E_0^0(N)$ as a function of system size N for the transverse Ising chain with free ends (15): $J_1 = 1$, $\Delta = 0$, $|J_2 - J_3| = 0, 0.2, 0.4, \dots, 4$ from top to bottom.

$$= \frac{1}{N(N+1)}(NE_0^0(N) - (N+1)E_0^0(N-1) - E_0^1(1)) < 0. \quad (\text{A.4})$$

Consequently, it is clear that

$$\Delta e_0(N) = \frac{1}{(N+1)(N+2)}((N+1)E_0^0(N+1) - (N+2)E_0^0(N) - E_0^1(1)) < 0, \quad (\text{A.5})$$

if $E_0^0(N+1) - 2E_0^0(N) + E_0^0(N-1) \leq 0$, i.e. the ground state energy of finite transverse Ising chain is a convex function of N . The last condition is ensured by non-increasing $\Delta E_0^0(N) = E_0^0(N+1) - E_0^0(N)$ ($\Delta E_0^0(N) \geq \Delta E_0^0(N+1)$) that can be shown by numerical calculations for finite chains (see figure A1) using the numerical approach [65]. For $J_2 = J_3$ we get the free spin Hamiltonian and $E_0^0(N)$ depends linearly on N . Conditions (A.4),(A.5) together mean that $e_0(N, 1)$ may have only one extremum and it is the maximum. Therefore, $e_0(N, 1)$ may take the minimal value only in two limiting cases $N = 1$, $N \rightarrow \infty$. The same result can be analogously obtained for $e_0(N, 2)$. Now we can compare the energies of $(N, 1)$ and $(N, 2)$ configurations. For $|h| \geq \frac{J_1+J_2}{2}$

$$e_0(1, 1) - e_0(1, 2) = \frac{1}{6} \left(-\frac{J_1(1+\Delta)}{2} - (J_2 + J_3) + |h| \right) < 0, \quad (\text{A.6})$$

due to the upper boundary of condition (21). To summarize, the ground state configuration in the region confined by (21) can correspond to either staggered bond or uniform purity configuration.

Let us consider the ground state for $|h| > J_2 + J_3 + \frac{J_1(1+\Delta)}{2}$. Similarly to the previous case we can prove that $e_0(N, M)$ is a convex function of N and M if the ground state energies of the uniform chains have the following properties:

$$\begin{aligned} E_0^0(N+1) - 2E_0^0(N) + E_0^0(N-1) &\leq 0, \\ E_0^1(N+1) - 2E_0^1(N) + E_0^1(N-1) &\leq 0. \end{aligned} \quad (\text{A.7})$$

One can find that $E_0^1(N+1) - E_0^1(N) = \frac{|J_2 - J_3|}{4}$, and $E_0^1(N+1) - 2E_0^1(N) + E_0^1(N-1) = 0$. That is why the minimal value of the ground state can be achieved in one of three cases: staggered bond, purity and impurity configuration. The staggered bond configuration should be excluded from this list for $|h| > J_2 + J_3 + \frac{J_1(1+\Delta)}{2}$, since it cannot be the ground state due to the variational principle.

References

- [1] Lacroix C, Mendels P, Mila F (ed) 2011 *Introduction to Frustrated Magnetism (Springer series in Solid-state Science vol 164)* (Berlin Heidelberg: Springer-Verlag)
- [2] Schollwöck U, Richter J, Farnell D J J, Bishop R F (ed) 2004 *Quantum Magnetism*, (Lecture Notes in Physics vol 645) (Berlin: Springer)
- [3] Miyahara S 2011 *Introduction to Frustrated Magnetism (Springer series in Solid-state Science vol 164)* ed Lacroix C, Mendels P, Mila F (Berlin Heidelberg: Springer-Verlag) pp 513-536
- [4] Kumar B 2002 *Phys. Rev. B* **66** 024406
- [5] Schmidt H-J 2005 *J. Phys. A: Math. Gen.* **38** 2123
- [6] Gellé A, Läuchli A M, Kumar B, Mila F 2008 *Phys. Rev. B* **77** 014419
- [7] Schmidt H-J, Richter J 2010 *J. Phys. A: Math. Theor.* **43** 405205
- [8] Derzhko O, Richter J, Honecker A, Schmidt H-J 2007 *Fizika Nizkikh Temperatur* **33** 982 [*Low Temp. Phys.* **33** 745].
- [9] Barry J H, Meisel M W 1998 *Phys. Rev. B* **58** 3129;
Barry J H, Cohen J D, Meisel M W 2009 *Int. J. Mod. Phys. B* **23** 1981
- [10] Batchelor M T, Guan X W, Oelkers N, Ying Z-J 2004 *J. Stat. Phys.* **116** 571;
Batchelor M T, Guan X W, Oelkers N, Tsuboi Z 2007 *Adv. Phys.* **56** 465
- [11] Strečka J 2010 *Phys. Lett. A* **374** 3718
- [12] Čanová L, Strečka J, Jaščur M 2006 *J. Phys.: Condens. Matter* **18** 4967
- [13] Lieb E, Schultz T, and Mattis D 1961 *Ann. Phys. (N.Y.)* **16** 407
- [14] Brzezicki W, Oleś A M 2009 *Phys. Rev. B* **80** 014405
- [15] Brzezicki W, Oleś A M 2010 *J. Phys.: Conf. Ser.* **200** 012017
- [16] Brzezicki W 2010 *AIP Conf. Proc.* **1297** 407
- [17] Dagotto E, Rice T M 1996 *Science* **271** 618
- [18] Dagotto E 1999 *Rep. Prog. Phys.* **62** 1525
- [19] Legeza Ö, Fáth G, Sólyom J 1997 *Phys. Rev. B* **55** 291
- [20] Legeza Ö, Sólyom J 1997 *Phys. Rev. B* **56** 14449
- [21] Wang X 2000 *Mod. Phys. Lett.* **14** 327
- [22] Honecker A, Mila F, Troyer M 2000 *Eur. Phys. J. B* **15** 227
- [23] Okazaki N, Miyoshi J, Sakai T 2000 *J. Phys. Soc. Jpn.* **69** 37
- [24] Sakai T, Okazaki N 2000 *J. Appl. Phys.* **87** 5893
- [25] Chandra V R, Surendran N 2006 *Phys. Rev. B* **74** 024421
- [26] Zheng Weihong, Kotov V, Oitmaa J 1998 *Phys. Rev. B* **57** 11439
- [27] Totsuka K 1998 *Phys. Rev. B* **57** 3454
- [28] Kim E H, Sólyom J 1999 *Phys. Rev. B* **60** 15230
- [29] Allen D, Essler F H L, Nersisyan A A 2000 *Phys. Rev. B* **61** 8871
- [30] Mila F 1998 *Eur. Phys. J. B* **6** 201
- [31] Kim E H, Legeza Ö, Sólyom J 2008 *Phys. Rev. B* **77** 205121
- [32] Starykh O A, Balents L 2004 *Phys. Rev. Lett.* **93** 127202
- [33] Hikihara T, Starykh O A, 2010 *Phys. Rev. B* **81** 064432
- [34] Michaud F, Coletta T, Manmana S R, Picon J-D, Mila F 2010 *Phys. Rev. B* **81** 014407
- [35] Gelfand M P 1991 *Phys. Rev. B* **43** 8644
- [36] Xian Y 1995 *Phys. Rev. B* **52** 12485

- [37] Brehmer S, Kolezhuk A K, Mikeska H-J, Neugebauer U 1998 *J. Phys.: Condens. Matter* **10** 1103
- [38] Kolezhuk A K, Mikeska H-J 1998 *Int. J. Mod. Phys. B* **12** 2325
- [39] Ramakko B, Azzouz M 2007 *Phys. Rev. B* **76** 064419
- [40] Azzouz M, Ramakko B 2008 *Can. J. Phys.* **86** 509
- [41] Ramakko B, Azzouz M 2008 *Can. J. Phys.* **86** 1125
- [42] Hiroi Z, Azuma M, Takano M, Bando Y 1991 *J. Solid State Chem.* **95** 230
- [43] Azuma M, Hiroi Z, Takano M, Ishida K, Kitaoka Y 1994 *Phys. Rev. Lett.* **73** 3463
- [44] Chiari B, Piovesana O, Tarantelli T, Zanazzi P F 1990 *Inorg. Chem.* **29** 1172
- [45] Chaboussant G, Julien M-H, Fagot-Revurat Y, Lévy L P, Berthier C, Horvatič M, Piovesana O 1997 *Phys. Rev. Lett.* **79** 925
- [46] Chaboussant G, Crowell P A, Lévy L P, Piovesana O, Madouri A, Dailly D 1997 *Phys. Rev. B* **55** 3046
- [47] Chaboussant G, Fagot-Revurat Y, Julien M-H, Hanson M E, Berthier C, Morvatič M, Lévy L P, Piovesana O 1998 *Phys. Rev. Lett.* **80** 2713
- [48] Watson B C, Kotov V N, Meisel M W, Hall D W, Granroth G E, Montfrooij W T, Nagler S E, Jensen D A, Backov R, Petruska M A, Fanucci G E, Talham D R 2001 *Phys. Rev. Lett.* **86** 5168
- [49] Landee C P, Turnbull M M, Galeriu C, Giantsidis J, Woodward F M 2001 *Phys. Rev. B* **63** 100402
- [50] Shiramura W, Takatsu K, Tanaka H, Kamishima K, Takahashi M, Mitamura H, Goto T 1997 *J. Phys. Soc. Jpn.* **66** 1900
- [51] Oosawa A, Takamasu T, Tatani K, Abe H, Tsujii N, Suzuki O, Tanaka H, Kido G, Kindo K 2002 *Phys. Rev. B* **66** 104405
- [52] Oosawa A, Katori H A, Tanaka H 2001 *Phys. Rev. B* **63** 134416
- [53] Oosawa A, Fujisawa M, Osakabe T, Kakurai K, Tanaka H 2003 *J. Phys. Soc. Jpn.* **72** 1026
- [54] Matsumoto M, Normand B, Rice T M, Sigrist M 2002 *Phys. Rev. Lett.* **89** 077203
- [55] Maekawa S 1996 *Science* **273** 1515
- [56] Leonowicz M E, Johnson J W, Brody J F, Shannon H F, Newsam J M 1985 *J. Solid St. Chem.* **56** 370
- [57] Korotin M A, Anisimov V I, Saha-Dasgupta T, Dasgupta I 2000 *J. Phys.: Condens. Matter* **12** 113
- [58] Katoh K, Hosokoshi Y, Inoue K 2000 *J. Phys. Soc. Jpn.* **69** 1008
- [59] Hosokoshi Y, Katoh K, Markosyan A S, Inoue K 2001 *Synthetic Metals* **121** 1838
- [60] Katsura S 1963 *Phys. Rev.* **127** 1508
- [61] Pfeuty P 1970 *Ann. Phys. (N.Y.)* **57** 79
- [62] Baxter R J 1982 *Exactly Solved Models in Statistical Mechanics* (London: Academic Press)
- [63] Bose I, Gayen S 1993 *Phys. Rev. B* **48** 10653
- [64] Shastry B S, Sutherland B 1981 *Physica B* **108** 1069; 1981 *Phys. Rev. Lett.* **47** 964
- [65] Derzhko O, Krokhmalkii T 1997 *Phys. Rev. B* **56** 11659